# A Pair of Oviduct-Born *Pickpocket* Neurons Important for Egg-Laying in *Drosophila melanogaster*

**Hyunjin Lee[1,2], Hyun Woo Choi[1,2], Chen Zhang[1], Zee-Yong Park[1,\*], and Young-Joon Kim[1,\*]**

During copulation, male *Drosophila* transfers Sex Peptide (SP) to females where it acts on internal sensory neurons expressing *pickpocket* (*ppk*). These neurons induce a post-mating response (PMR) that includes elevated egg-laying and refractoriness to re-mating. Exactly how *ppk* neurons regulate the different aspects of the PMR, however, remains unclear. Here, we identify a small subset of the *ppk* neurons which requires expression of a pre-mRNA splicing factor CG3542 for egg-laying, but not refractoriness to mating. We identify two *CG3542-ppk* expressing neurons that innervate the upper oviduct and appear to be responsible for normal egg-laying. Our results suggest specific subsets of the *ppk* neurons are responsible for each PMR component.

## INTRODUCTION

Egg-laying is a key reproductive behavior in many invertebrates that depends on the coordinated action of multiple physiological and behavioral steps associated with egg formation, ovulation, and oviposition. Like reproduction in mammals, each step of egg-laying is influenced by endocrine factors; juvenile hormone (JH) is required for egg formation (Bownes, 1989; Gruntenko et al., 2010; Sliter et al., 1987), and octopamine is required for ovulation (Monastirioti, 1996; 2003; Rodri et al., 2006). Even neurons producing Insulin-like peptide 7 (*Ilp7*) have been linked to oviposition in *Drosophila melanogaster* (Yang et al., 2008).

As with many other animals, egg-laying in *Drosophila* is tightly associated with mating. After a female mates and receives sperm from a male, she becomes refractory to further mating and begins to lay eggs. This behavioral switch, which is known as the post-mating response (PMR), is induced by Sex Peptide (SP) in the seminal fluid transferred to females during insemination (Aigaki and Fleischmann, 1991; Chen et al., 1988; Liu and Kubli, 2003). Females that mate with males lacking SP lay few

eggs and mate multiple times (Peng et al., 2005a). SP is also associated with other behavioral and physiological changes, such as feeding, sleep and immune responses (Carvalho et al., 2006; Domanitskaya et al., 2007; Isaac et al., 2010; Peng et al., 2005b; Ribeiro and Dickson, 2010; Walker et al., 2015).

SP acts via a G-protein coupled receptor called SP receptor (SPR) (Yapici et al., 2008). SPR expression in *pickpocket (ppk)* neurons is required for a normal PMR, and the activation of SPR in *ppk* neurons is sufficient to induce the PMR even in virgin flies. The female genital tract houses 30-38 *ppk* neurons. Silencing of these neurons induces a PMR similar to that caused by mating or SPR activation. This indicates activation of SPR suppresses the activity of the *ppk* neurons (Häsemeyer et al., 2009; Yang et al., 2009). ppk is co-expressed in female reproductive organs with *fruitless (fru)* and/or *doublesex (dsx)*, two genes encoding transcription factors important for sex determination (Häsemeyer et al., 2009; Rezával et al., 2012; Yang et al., 2009). The *ppk* gene encodes an amiloride-sensitive sodium channel important for mechanosensation (Adams et al., 1998; Zhong et al., 2010). Because of this, peripheral neurons in the legs, wings, and genital tract that express *ppk* are generally considered sensory neurons that signal to the central brain. Still, even though SP and SPR in *ppk* neurons clearly direct the various components of the PMR, it is unclear which *ppk* neurons regulate the distinct behaviors of mating receptivity and egg-laying.

As a GPCR, SPR appears to be coupled with $G\alpha i$ or $G\alpha o$, both of which reduce levels of the intracellular second messenger cAMP (Yapici et al., 2008). This drop in cAMP, in turn, modulates the activity of cAMP-dependent protein kinase A (PKA). Thus, we reasoned SPR activation should result in global changes in the phosphorylation state of many proteins, including important mediators downstream of SPR. In this study, we took a mass spectrometry-based proteomic approach to identify phosphoproteins downstream of SPR signaling. After identifying proteins whose phosphorylation status changes in response to SP treatment, we examined the functions of these proteins using RNAi. We found that *CG3542* (Mount and Salz, 2000; Zhu et al., 2005), which encodes a protein closely related to the pre-mRNA processing factor PRP40, is important in *ppk* neurons for the increase in egg-laying of mated females but not for their reduced mating receptivity. Using an intersectional genetic approach, we identified a group of 2-3 *ppk* and *CG3542* double-positive neurons that innervate the upper oviduct. Silencing of these neurons affects egg-laying but not mating receptivity in mated females. Our results suggest egg-laying and mating receptivity are regulated by distinct subsets of *ppk* neurons.

[1]School of Life Sciences, Gwangju Institute of Science and Technology, Gwangju 61005, Korea, [2]These authors contributed equally to this work.
*Correspondence: kimyj@gist.ac.kr (YJK); zeeyong@gist.ac.kr (ZYP)

# MATERIALS AND METHODS

## Phosphoprotein analysis

BG2 cells were obtained from Drosophila Genome Resource Center (Cell line stock number, 51), and cultured according to the protocol form the provider (https://dgrc.bio.indiana.edu/include/file/general_maintenance.pdf). BG2 cells with or without SP treatment were lysed in protein extraction buffer containing 50mM Tris-HCl pH 8.2, 8 M Urea, 75 mM NaCl, 1 mM NaF, 1 mM β-glycerophosphate, 1mM sodium orthovanadate, 1 mM sodium pyrophosphate and 1 mM PMSF. After sonication, protein concentrations were determined using a BCA Protein Assay Kit (Thermo Scientific, UK). Protein samples (100 µg each) were chemically reduced (5 mM, DTT) and alkylated (25 mM, IAA) prior to trypsin digestion. After 4-fold dilution with 25 mM Tris-HCl buffer (pH 8.2), the protein samples were enzymatically digested using a sequencing grade trypsin at an enzyme to substrate ratio of 1:50 at 37°C for 16 h. Digestion reaction was stopped by the addition of 90% formic acid to a final concentration of 1%. Resulting tryptic digest peptide samples were desalted for subsequent phosphopeptide enrichment procedure. Phosphopeptides enriched with IMAC POROS 20 MC were subsequently subjected to the micro RPLC-MS/MS analysis described previously (Choi et al., 2011). Briefly, analyses of phosphopeptide-enriched samples were performed using Agilent 1100 Series high-performance liquid chromatography (HPLC) (Agilent Technologies) coupled to a linear quadrupole ion trap mass spectrometer (LTQ, Thermo Finnigan, USA). The resulting MS/MS spectra searched against a composite protein database containing the IPI mouse protein database (v.3.28), and its reversed complement using SEQUEST algorithm (Sorcerer system). Differential modification search options for phosphorylation modification (+80 on Ser, Thr, Tyr), and oxidation (+16 on Met), were considered in the search. 'Peptide prophet' and 'Protein prophet' scores of 90% was used to filter the search results. We applied the log2(protein ratio) from relative spectral counts (Rsc) for label free quantification (Old et al., 2005). $RSC = \log2[(n2 + f)/(n1 + f)] + \log2[(t1 - n1 + f)/(t2 - n2 + f)]$ where, for each protein, RSC is the log2 ratio of abundance between Samples 1 and 2; $n1$ and $n2$ are spectral counts for the protein in Samples 1 and 2, respectively; $t1$ and $t2$ are total numbers of spectra over all proteins in control and SP-treated samples; and $f$ is a correction factor, set to 0.5 (Beissbarth et al., 2004). Ammonium bicarbonate, calcium chloride, dithiothreitol (DTT), iodoacetamide (IAA), sodium chloride, sodium orthovanadate ($Na_3VO_4$), sodium fluoride (NaF), phenylmethylsulfonyl fluoride (PMSF), sodium β-glycerophosphate, urea and ammonium dihydrogen phosphate ($NH_4H_2PO_4$) were purchased from Sigma (USA). Formic acid (FA) and trifluoroacetic acid (TFA) were obtained from Merck (Germany). HPLC grade acetonitrile (ACN), methanol and deionized water were all purchased from Fisher Science. Sequencing grade modified trypsin was obtained from Promega (USA). Aqua C18 (particle size 5 µm) reversed-phase column material was purchased from Phenomenx (USA). The IMAC POROS 20 MC was purchased from Applied Biosystems (USA).

## Fly strains

We obtained the following RNAi transgenic lines from the Vienna Drosophila RNAi Center (VDRC) (Austria): *CG14939-IR1* (VDRC stock number 107010), *CG6983-IR1* (35159), *CG5643-IR1* (27470), *CG3333-IR1* (34597), *CG8594-IR1* (4642), *CG8201-IR1* (52553), *CG11621-IR1* (16240), *CG3542-IR1* (26227), *CG3542-IR2* (26229), *CG10480-IR1* (38389), *CG2173-IR1* (36516), *CG8108-IR1* (35343), *CG11417-IR1* (18087), *CG4236-IR1* (26455), *CG6831-IR1* (40399), *CG33979-IR1* (21995), *CG31678-IR1* (103705), *CG6338-IR1* (12633), *CG10033-IR1* (38320), *CG42250-IR1* (33799), *CG3696-IR1* (10762), *CG6418-IR1* (40379), *CG9191-IR1* (52549), *CG30122-IR1* (106984), *CG16973-IR1* (101517), *CG2691-IR1* (110718), *CG6501-IR1* (105605), *CG14616-IR1* (106973), *CG8092-IR1* (28196), and *CG42783-IR1* (105624). Y. Jan (UCSF) provided *ppk-Gal4.* We combined *ppk-GAL4* with *UAS-Dicer2* and used it as a *ppk*-specific driver for all the RNAi experiments. B.J. Dickson kindly provided *UAS>stop>nSyb-GFP, UAS>stop>DSCAM17.1-GFP* and *UAS>stop>Kir2.1.* We also used the published lines *UAS>stop>mCD8-GFP* (Yu et al., 2010)*; LexAop-FLP* (Bussell et al., 2014) and *UAS-mSP* (Nakayama et al., 1997) in this study. To generate *CG3542-LexA* and *CG3542-GAL4*, we performed a PCR amplification of the genomic region 5′ of the CG3542 transcriptional start site (+228 to -22) (forward primer, 5′ NNGCGGCCGCCGATAA CAGAAAATCTACCGGGT-3′; reverse primer, 5′-NNTCTAGA CCCACGCTAGGAGGAACATT-3′) and cloned the product into the pENTR vector (Invitrogen). We then recombined this into the pBPnlsLexAp65Uw vector for the LexA line or the pPTGAL4(+) vector for the GAL4 line (Pfeiffer et al., 2010). We injected each final plasmid into embryos using standard techiniqes for insertion into a specific site on the second chromosome (*VIE-72A*) using phiC31-mediated recombination.

## Behavioral assays

We raised all flies on normal fly food at 25°C under a 12 h: 12 h light: dark cycle (Park et al., 2014). For all behavioral assays, we collected flies immediately after eclosion and aged females 3-5 days in groups of ~10 and males 4 days individually. For the initial mating assays, we paired virgin females individually with naïve Canton S (CS) males in 1 cm diameter chambers and counted the number of mating pairs for 1 h. In case of egg-laying, we transferred individual females who copulated within 1 h to vials containing normal fly food. Then, we counted the eggs laid by each female over the course of 48 h. For virgin egg-laying, we transferred 5 aged virgin females to vials containing normal fly food and counted the total eggs laid over the course of 48 h. For re-mating, we paired individual females who had mated within the past 48 h with naïve CS males and observed their mating for 1 h. All behavioral assays were performed at RT (25°C) and 60% humidity.

## Immunohistochemistry

We dissected ovaries in phosphate buffered saline (PBS) (pH 7.4) and fixed them in 4% paraformaldehyde in PBS for 30 min at room temperature. After washing them with PBST, we incubated them with a rabbit anti-GFP antibody (1:1000; Invitrogen, A11122) for 48 h at 4°C. After washing, we then incubated the samples for 24 h at 4°C with an Alexa 488-conjugated goat anti-rabbit (1:1000; Invitrogen, A11008) secondary antibody and an Alexa 555-conjugated phalloidin (1:1000; Invitrogen, A34055) to visualize actin in the muscle-rich reproductive tract. Finally, we mounted the tissues in Vectashield and imaged them with an LSM 700/Axiovert 200M confocal microscope (Zeiss). All confocal images are maximal intensity Z-projections. We performed all image processing with ImageJ.

## Statistics

We used GraphPad Prism 5 to compare experimental groups with multiple control groups using the ANOVA followed by Tukey's test for multiple comparisons.
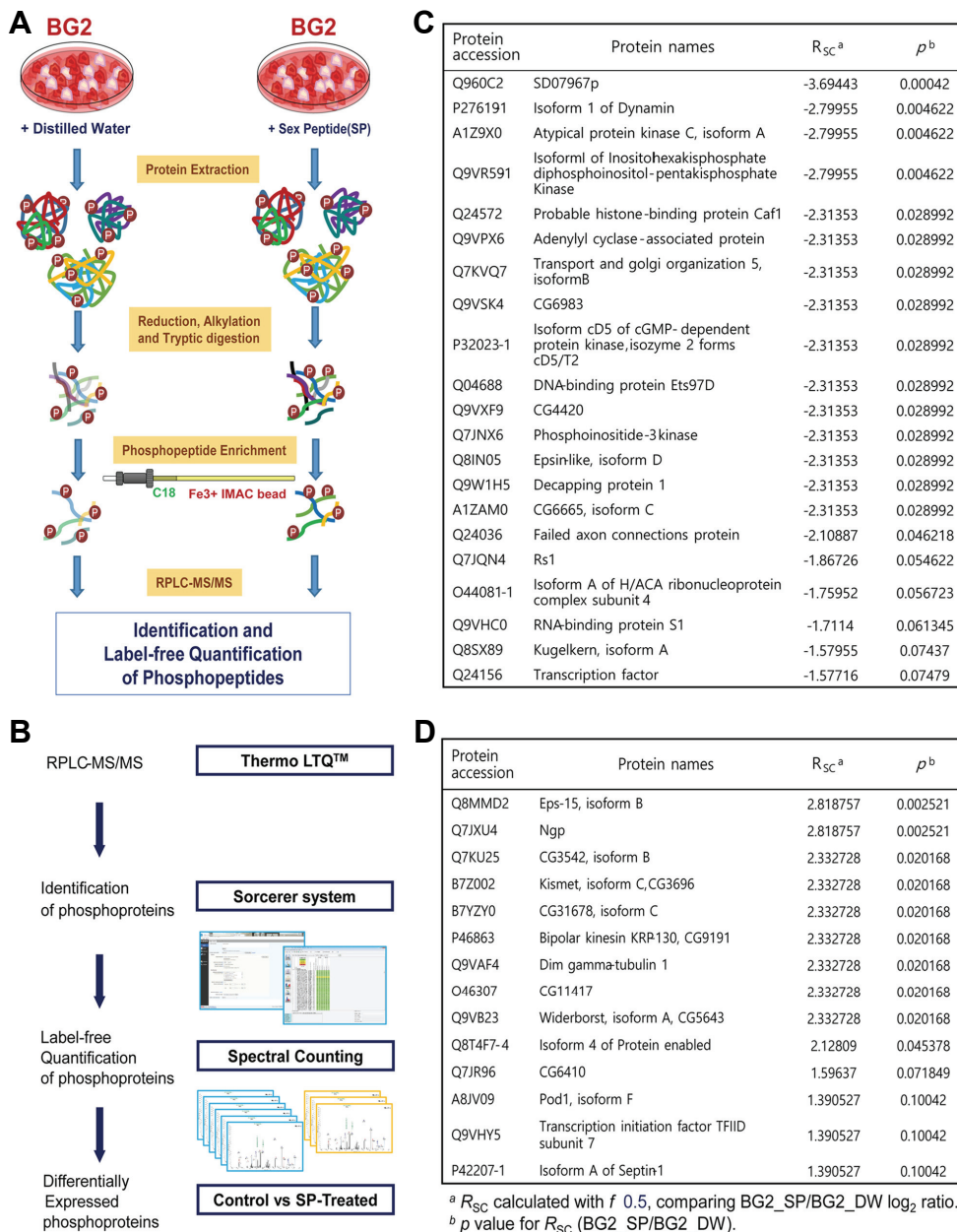
**Fig. 1.** Identification of signaling molecules downstream of SPR via a mass spectrometry-based label-free phosphoproteomic approach. (A) Experimental scheme for phosphopeptide enrichment. (B) Experimental scheme for micro RPLC-MS/MS analysis and label-free quantification. (C) Proteins showing reduced levels of phosphorylation in SP-treated BG2 cells as filtered by $R_{SC}$ significance ($p < 0.1$). (D) Proteins showing elevated levels of phosphorylation in SP-treated BG2 cells as filtered by $R_{SC}$ significance ($p < 0.1$).

**C**

| Protein accession | Protein names | $R_{SC}$[a] | $p$[b] |
|---|---|---|---|
| Q960C2 | SD07967p | -3.69443 | 0.00042 |
| P276191 | Isoform 1 of Dynamin | -2.79955 | 0.004622 |
| A1Z9X0 | Atypical protein kinase C, isoform A | -2.79955 | 0.004622 |
| Q9VR591 | Isoforml of Inositohexakisphosphate diphosphoinositol-pentakisphosphate Kinase | -2.79955 | 0.004622 |
| Q24572 | Probable histone-binding protein Caf1 | -2.31353 | 0.028992 |
| Q9VPX6 | Adenylyl cyclase-associated protein | -2.31353 | 0.028992 |
| Q7KVQ7 | Transport and golgi organization 5, isoformB | -2.31353 | 0.028992 |
| Q9VSK4 | CG6983 | -2.31353 | 0.028992 |
| P32023-1 | Isoform cD5 of cGMP-dependent protein kinase,isozyme 2 forms cD5/T2 | -2.31353 | 0.028992 |
| Q04688 | DNA-binding protein Ets97D | -2.31353 | 0.028992 |
| Q9VXF9 | CG4420 | -2.31353 | 0.028992 |
| Q7JNX6 | Phosphoinositide-3 kinase | -2.31353 | 0.028992 |
| Q8IN05 | Epsin-like, isoform D | -2.31353 | 0.028992 |
| Q9W1H5 | Decapping protein 1 | -2.31353 | 0.028992 |
| A1ZAM0 | CG6665, isoform C | -2.31353 | 0.028992 |
| Q24036 | Failed axon connections protein | -2.10887 | 0.046218 |
| Q7JQN4 | Rs1 | -1.86726 | 0.054622 |
| O44081-1 | Isoform A of H/ACA ribonucleoprotein complex subunit 4 | -1.75952 | 0.056723 |
| Q9VHC0 | RNA-binding protein S1 | -1.7114 | 0.061345 |
| Q8SX89 | Kugelkern, isoform A | -1.57955 | 0.07437 |
| Q24156 | Transcription factor | -1.57716 | 0.07479 |

**D**

| Protein accession | Protein names | $R_{SC}$[a] | $p$[b] |
|---|---|---|---|
| Q8MMD2 | Eps-15, isoform B | 2.818757 | 0.002521 |
| Q7JXU4 | Ngp | 2.818757 | 0.002521 |
| Q7KU25 | CG3542, isoform B | 2.332728 | 0.020168 |
| B7Z002 | Kismet, isoform C,CG3696 | 2.332728 | 0.020168 |
| B7YZY0 | CG31678, isoform C | 2.332728 | 0.020168 |
| P46863 | Bipolar kinesin KRP-130, CG9191 | 2.332728 | 0.020168 |
| Q9VAF4 | Dim gamma-tubulin 1 | 2.332728 | 0.020168 |
| O46307 | CG11417 | 2.332728 | 0.020168 |
| Q9VB23 | Widerborst, isoform A, CG5643 | 2.332728 | 0.020168 |
| Q8T4F7-4 | Isoform 4 of Protein enabled | 2.12809 | 0.045378 |
| Q7JR96 | CG6410 | 1.59637 | 0.071849 |
| A8JV09 | Pod1, isoform F | 1.390527 | 0.10042 |
| Q9VHY5 | Transcription initiation factor TFIID subunit 7 | 1.390527 | 0.10042 |
| P42207-1 | Isoform A of Septin-1 | 1.390527 | 0.10042 |

[a] $R_{SC}$ calculated with $f$ 0.5, comparing BG2_SP/BG2_DW $\log_2$ ratio.
[b] $p$ value for $R_{SC}$ (BG2_SP/BG2_DW).

## RESULTS

In this study, we hoped to discover proteins downstream of SP and SPR actions as well as the neurons that express them. To apply our mass spectrometry-based phospho-proteomic approach, we needed a cell line that expresses SPR. After examining several cell lines derived from *Drosophila* melanogaster nervous tissue, we found that the BG2 cell line derived from third instar larval brains meets this criterion (data not shown). After treating BG2 cells with 100 nM SP for 2 h, we analyzed them with label-free quantitative mass spectrometry. This technique permits the unbiased monitoring of protein phosphorylation levels at specific individual phosphorylation sites. We identified 35 proteins that show significantly different levels of phosphorylation between SP- and vehicle-treated cells ($p < 0.1$). Consistent with our prediction that SPR activation would reduce PKA activity, we found more proteins with reduced phosphorylation (21) than increased phosphorylation (14) (Fig. 1).

To determine whether any of these proteins showing altered phosphorylation upon SPR activation affect the egg-laying or mating refractoriness components of the PMR *in vivo*, we performed a small-scale RNAi screen knocking-down each candidate in *ppk* neurons (Fig. 2A). In this screen, we found females expressing *CG3542-IR1* show significantly elevated egg-laying for 48 h post-mating (Fig. 2B). Although knock-down of *CG3542* affects egg-laying, it does not seem to affect receptiv-
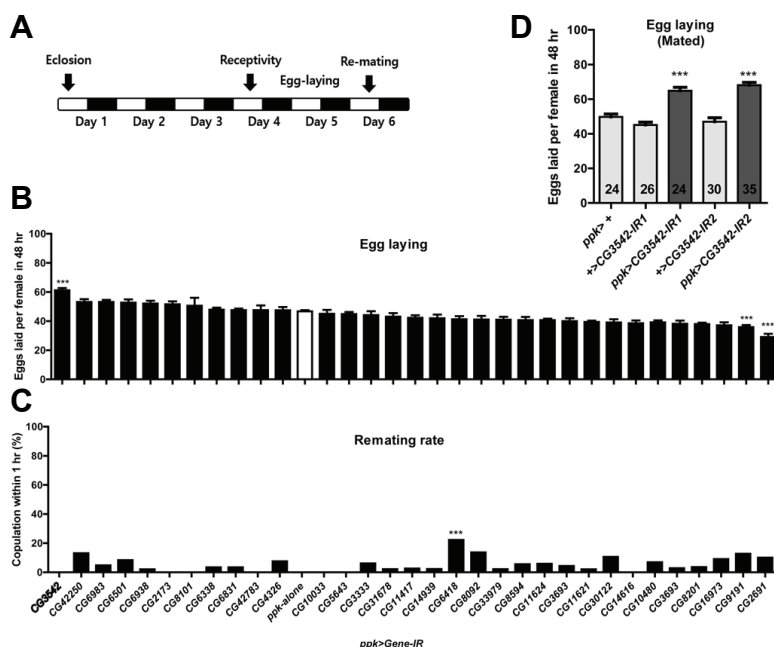
**Fig. 2.** CG3542 knock-down in *ppk* neurons affects egg-laying in mated females. (A) Behavioral protocol used for (B, C). (B) Eggs laid per female of the indicated *UAS* line crossed with *ppk-Gal4* for 48 h post-mating, *n* = 20-58 (n of *CG8101-RNAi* =12). ***p* < 0.001 for comparisons against *ppk-GAL4* alone (white bar); one-way ANOVA followed by Tukey's test for multiple comparisons. (C) Re-mating rate, *n* = 20-58 (*CG47283-RNAi* haven't be tested). ****p* < 0.001 for comparisons against *ppk-GAL4* alone; Fisher's exact test. (D) Eggs laid per female of the indicated genotype for 48 h post-mating, *n* = 20-35. ****p* < 0.001, one-way ANOVA followed by Tukey's test for multiple comparisons.

ity to re-mating 48 h after initial mating (Fig. 2C). We confirmed the specificity of the RNAi-mediated knock-down of CG3542 by testing an additional RNAi line (*CG3542-IR2*) and observed a similar effect on egg-laying (Fig. 2D). This suggests CG3542 is important for the function of *ppk* neurons, especially the subset of the *ppk* neurons that direct post-mating changes in egg-laying. *CG3542* encodes a protein predicted to regulate mRNA splicing, but this has not yet been confirmed.

Since knock-down of CG3542 in *ppk* neurons affects egg-laying but not re-mating, we reasoned that we should be able to affect egg-laying by manipulating the activity of *ppk* neurons positive for CG3542. To test this idea, we adopted an intersectional genetic approach. We generated a *CG3542-LexA* transgene (Fig. 3A) and combined it with *LexAOP-FLP, ppk-GAL4*, and *UAS-FRT-stop-FRT-Kir2.1*. In females carrying all of these transgenes, *CG3542-LexA* drives the expression of a flippase that removes the transcriptional stop cassette flanked by FRT sites (FRT-stop-FRT) in the UAS transgene. This means only cells expressing both *CG3542-LexA* and *ppk-GAL4* will produce Kir2.1, an inwardly-rectifying potassium channel (Johns and Marx, 1999) that suppresses neural depolarization (Fig. 3B). Indeed, although mated females with silenced *CG3542-LexA* and *ppk-GAL4* double-positive (henceforth, *CG3542-ppk*) neurons lay more eggs than controls (Fig. 3C), their virgin counterparts do not. The egg-laying phenotype in these females is comparable to that observed in *ppk>CG3542-IR* females. When we activated *CG3542-ppk* neurons using dTrpA1, a temperature-sensitive cation channel that depolarizes neurons at warmer temperatures (30°C), we observed no change in egg-laying (Fig. 3D). It is important to note that the silencing of all *ppk* neurons was previously reported to induce significant egg-laying even in virgin females (See also Fig. 3E). Since, in contrast, the silencing of *CG3542-ppk* neurons has no effect on virgin egg-laying, we have confirmed a role for *CG3542-ppk* neurons in specifically regulating post-mating egg-laying.

We next examined EGFP-expressing neurons in the genital

tract of females carrying *CG3542-LexA*, *LexAOP-FLP*, *ppk-GAL4*, and *UAS-FRT-stop-FRT-mCD8-EGFP*. Remarkably, we were only able to detect 2-3 EGFP-positive neurons per female genital tract (Fig. 3F): two in the lateral oviduct (Fig. 3F′) and one in the middle oviduct near the spermatheca (Fig. 3F″). The neurons in the lateral oviduct were paired in most preparations (*n* = 4/5), but the neurons in the common oviduct always appeared alone (*n* = 5/5). In most preparations, we were unable to detect any EGFP in the uterus (*n* = 4/5). To better understand the function of these *CG3542-ppk* neurons, we examined their polarity using the pre-synaptic marker nsyb-EGFP (Zhang et al., 2002) and the post-synaptic marker Dscam-GFP. We detected significant accumulation of nsyb-EGFP, but not Dscam-GFP in processes innervating the lateral oviduct. This indicates the *CG3542-ppk* neurons are likely efferent modulators of lateral oviduct contractility for controlling ovulation (Figs. 3G-3H).

Expression of a membrane-tethered SP (mSP) in either all neurons or specifically in *ppk* neurons suppresses mating and increases egg-laying in virgin females, recapitulating the post-mating response of mated females (Nakayama et al., 1997; Rezával et al., 2012; Yang et al., 2009). Since we found the *CG3542-ppk* neurons regulate egg-laying, we next asked whether driving expression of mSP in *CG3542* neurons also induces egg-laying in virgin females. To do so, we generated *CG3542-GAL4* flies using the same genomic fragment we used to generate *CG3542-LexA* (Fig. 3A). We confirmed *CG3542-GAL4* driving the expression of Kir2.1 affects the egg-laying of both mated and virgin females without affecting mating receptivity (Figs. 4A-4C). This indicates *CG3542-GAL4*, like *CG3542-LexA*, is expressed in neurons relevant to egg-laying. Finally, we combined *CG3542-GAL4* and *UAS-mSP* to express mSP in the *CG3542* neurons and compared their virgin egg-laying behavior with that of *ppk>mSP* flies. We confirmed that *ppk>mSP* virgins show elevated egg-laying compared to controls, but *CG3542>mSP* do not (Figs. 4D-4F). This suggests the presence of an unknown subset of *ppk* neurons in addition to the *CG3542-ppk* neurons that also regulates egg-laying.
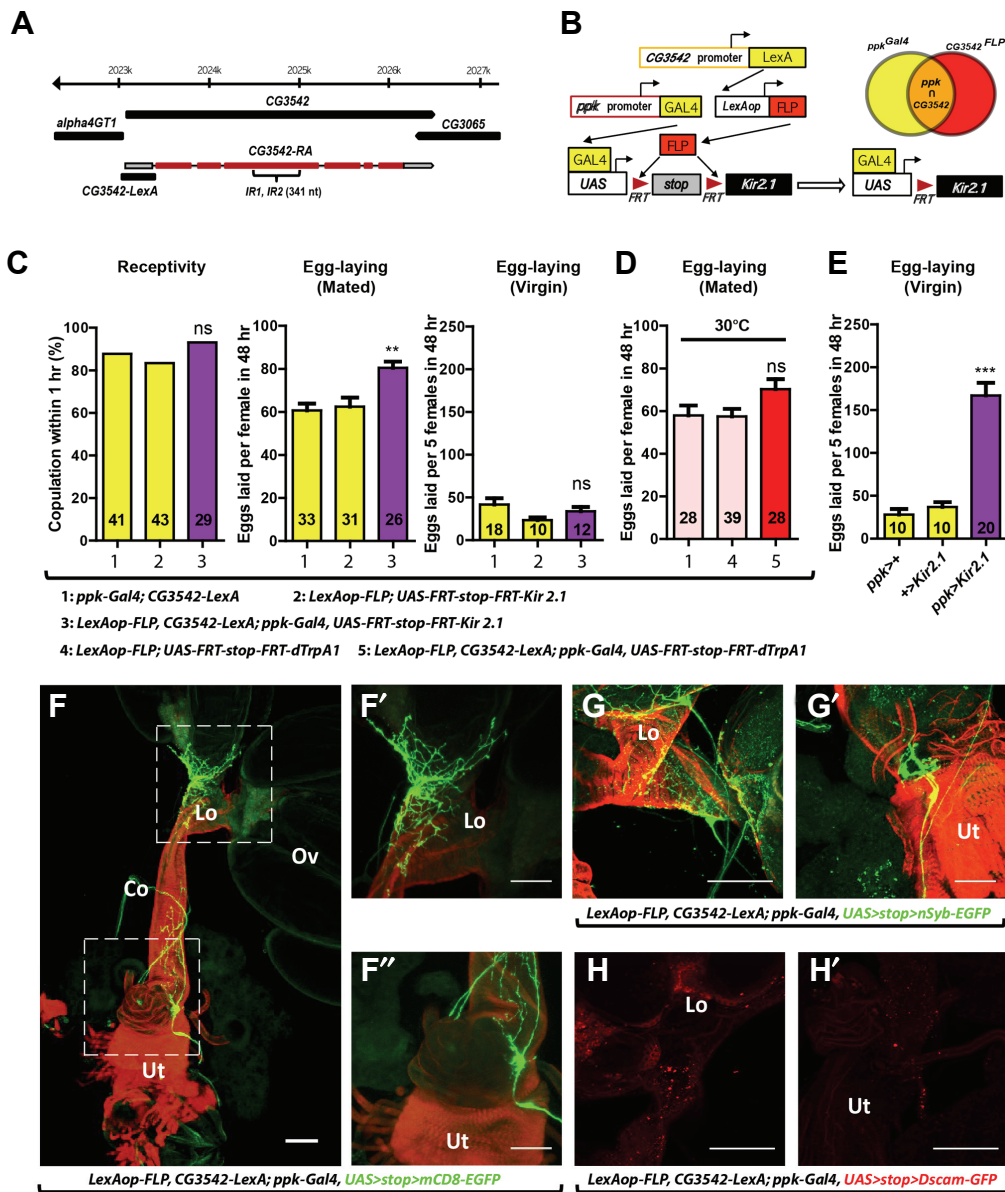
**Fig. 3.** *ppk-Gal4* and *CG3542-LexA* double positive neurons modulate egg-laying in mated females. (A) The CG3542 gene structure (top) and the genomic fragment used to generate CG3542-LexA (bottom). The gray and red boxes indicate untranslated and translated exons of the CG3542 transcript, respectively. (B) Schematic detailing our intersectional genetic approach. (C) Mating receptivity in virgin females (left), egg-laying by mated females (middle) and egg-laying by virgin females (right) of the indicated genotypes. For egg-laying, we counted eggs laid per mated female or per five virgin females for 48 h. The numbers inside each bar indicate *n*. Data are presented as mean percentages (for mating receptivity) or means ± SEM (for egg-laying). \*\**p* < 0.01, not significant (ns) *p* > 0.05 for comparisons against both controls (yellow bars); Fisher's exact test (mating receptivity); one-way ANOVA followed by Tukey's test for multiple comparisons (egg-laying). (D) Eggs laid per mated female of the indicated genotypes for 48 h. The numbers inside each bar indicate *n*. Data are presented as means ± SEM. Not significant (ns), *p* > 0.05 for comparisons against both controls (pink bars); one-way ANOVA followed by Tukey's test for multiple comparisons. (E) Eggs laid per five virgin females of the indicated genotypes for 48 h. The numbers inside each bar indicate *n*. Data are presented as means ± SEM. \*\*\**p* < 0.001 for comparisons against both controls (yellow bars); one-way ANOVA followed by Tukey's test for multiple comparisons. (F) Confocal images of reproductive organs from *ppk-Gal4 CG3542-LexA LexAop-FLP UAS>stop>mCD8-EGFP* females, stained with an anti-GFP (green) antibody and a fluorophore-conjugated phalloidin (red). Ov, ovary; Lo, lateral oviduct; Co, common oviduct; Ut, uterus. Scale bar, 100 μm. (F′ and F″) High magnification view of the areas outlined in (E). (G and G′) Visualization of the pre-synaptic marker nSyb-EGFP in *CG3542-ppk* neurons from females carrying *ppk-Gal4, CG3542-LexA, LexAop-FLP,* and *UAS>stop>nSyb-EGFP*, stained with an anti-GFP (green) antibody and a fluorophore-conjugated phalloidin (red). (F), the lateral oviduct. (F′), the common oviduct. Scale bar, 100 μm. (H and H′) Visualization of the post-synaptic marker Dscam-GFP in *CG3542-ppk* neurons from females carrying *ppk-Gal4, CG3542-LexA, LexAop-FLP,* and *UAS>stop>Dscam-GFP*, stained with an anti-GFP (red) antibody and the color was presented in red. (G), the lateral oviduct. (G′), the common oviduct. Scale bar, 100 μm.
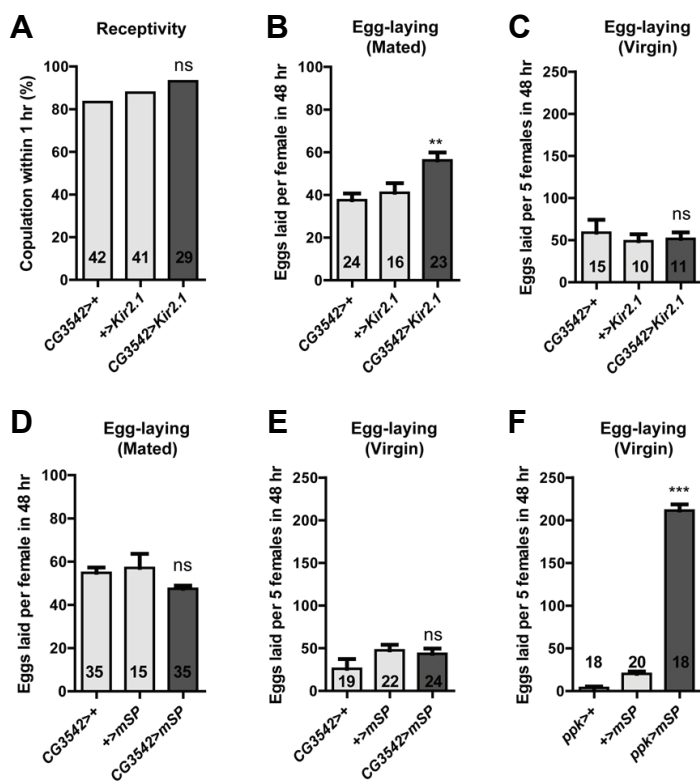
**Fig. 4.** SPR activation in *CG3542* neurons is insufficient for inducing egg-laying in virgin females. (A) Mating receptivity of virgin females of the indicated genotypes. The numbers inside each bar indicate *n*. Data are presented as mean percentages. Not significant (ns), $p > 0.05$ for comparisons against both controls (light gray bars); Fisher's exact test. (B, D) Eggs laid per female of the indicated genotypes for 48 h post-mating. The numbers inside each bar indicate *n*. Data are presented as means ± SEM. **$p < 0.01$ and not significant (ns), $p > 0.05$ for comparisons against both controls (light gray bars); one-way ANOVA followed by Tukey's test for multiple comparisons. (C, E, and F) Eggs laid per five virgin females of the indicated genotypes for 48 h. The numbers inside each bar indicate *n*. Data are presented as means ± SEM. ***$p < 0.001$ and not significant (ns), $p > 0.05$ for comparisons against both controls (light gray bars); one-way ANOVA followed by Tukey's test for multiple comparisons.

## DISCUSSION

Here, we have identified a small subset of *ppk* neurons that modulate egg-laying activity in female *Drosophila*. Using proteomic techniques we identified *CG3542* as a gene whose phosphorylation is enhanced by SP treatment. We found that expression of *CG3542* in *ppk* neurons is required to maintain normal levels of egg-laying. CG3542 encodes a protein homologous to the yeast pre-mRNA splicing factor 40 (PRP40), which associates with the U1 small nuclear ribonucleoprotein (snRNP) and bridges the 5′ and 3′ ends of spliced introns (Tang and Rosbash, 1996). Normal male courtship behavior was recently found to depend on the interaction between the P-element Somatic Inhibitor (PSI) and the U1 snRNP complex. This complex affects the alternative splicing of a list of roughly 1,200 genes, including the sexually dimorphic transcription factor *fruitless (fru)* that regulates gender-specific behaviors (Wang et al., 2016). Although it remains unclear whether the oviduct *CG3542-ppk* neurons are *fru*-positive, one pair of lateral oviduct ppk neurons expresses *fru*GAL4, a GAL4 knock-in at the *fru-P1* locus (Yang et al., 2009). Thus, we speculate that the knock-down of CG3542 in the *CG3542-ppk* neurons alters the splicing of genes important for their development and/or function.

SPR is a Gαi/Gαo-coupled GPCR. Its activation inhibits adenylate cyclase, reduces intracellular cAMP, and inhibits PKA. Thus, SPR activation should produce global changes in the phosphorylation states of many proteins, particularly substrates of PKA. Indeed, our analysis identified many proteins that become hypo-phosphorylated upon SP treatment. Unexpectedly, we also identified several proteins, including CG3542, that become hyper-phosphorylated. This means SPR can promote

protein phosphorylation as well as de-phosphorylation. Although the mechanism underlying this phenomenon remains unclear, it is likely SPR can affect downstream signaling pathways other than PKA. Consistent with this, over-expression in *ppk* neurons of an activated PKA affects mating receptivity much more strongly than it affects egg-laying (Yang et al., 2009). This suggests the distinct components of the PMR depend on distinct signaling pathways downstream of SPR. It is also of course possible that the hyper-phosphorylation of CG3542 induced by SPR activation is indirect.

Here, we report that the silencing of a small subset of ppk neurons increases post-mating egg-laying. Previously, Haesemeyer et al. (2009) found silencing all the ppk neurons has very little impact on post-mating egg-laying behavior. This discrepancy with our results may stem from a difference in the genetic reagents used to silence the *ppk* neurons. Haesemeyer et al. used the temperature-sensitive, dominant-negative dynamin mutant shi^ts to conditionally block the recycling of neurotransmitter vesicles at the restrictive temperatures (Kitamoto, 2001). We, instead chose the inward-rectifying potassium channel Kir2.1 to achieve much stronger silencing.

Previous studies have suggested mating receptivity and egg-laying are genetically separable in *Drosophila* (Yang et al., 2009). This is consistent with our observation that silencing only 2-3 *CG3542-ppk* neurons of the ~38 *ppk* neurons in the female genital tract affects egg-laying but not mating receptivity. Nevertheless, we found mSP expression in the *CG3542-ppk* neurons is insufficient to induce egg-laying in virgin females, unlike mSP expression in all *ppk* neurons. Egg-laying is the culmination of a multi-step process comprising egg-formation, ovulation, fertilization, and oviposition. The anatomy of the *CG3542-ppk* neurons suggests they may play a role only in ovulation, because

their pre-synaptic processes extensively innervate the basal domain of the lateral oviduct. This may explain why SPR activation in the 2-3 *CG3542-ppk* neurons cannot activate all steps of the process enough to increase egg-laying as a whole.

## ACKNOWLEDGMENTS

## REFERENCES

Adams, C.M., Anderson, M.G., Motto, D.G., Price, M.P., Johnson, W.A., and Welsh, M.J. (1998). Ripped pocket and pickpocket, novel Drosophila DEG/ENaC subunits expressed in early development and in mechanosensory neurons. J. Cell Biol. *140*, 143-152.

Aigaki, T., and Fleischmann, I. (1991). Ectopic expression of sex peptide reproductive behavior of female. Neuron *7*, 557-563.

Beissbarth, T., Hyde, L., Smyth, G.K., Job, C., Boon, W.-M., Tan, S.-S., Scott, H.S., and Speed, T.P. (2004). Statistical modeling of sequencing errors in SAGE libraries. Bioinformatics *20 Suppl 1*, i31-i39.

Bownes, M. (1989). The roles of juvenile hormone, ecdysone and the ovary in the controlof Drosophila vitellogenesis. J. Insect Physiol. *35*, 409-413.

Bussell, J.J., Yapici, N., Zhang, S.X., Dickson, B.J., and Vosshall, L.B. (2014). Abdominal-B neurons control Drosophila virgin female receptivity. Curr. Biol. *24*, 1584-1595.

Carvalho, G.B., Kapahi, P., Anderson, D.J., and Benzer, S. (2006). Allocrine modulation of feeding behavior by the sex peptide of Drosophila. Curr. Biol. *16*, 692-696.

Chen, P.S., Stumm-Zollinger, E., Aigaki, T., Balmer, J., Bienz, M., and Böhlen, P. (1988). A male accessory gland peptide that regulates reproductive behavior of female D. melanogaster. Cell *54*, 291-298.

Choi, H., Lee, S., Jun, C.-D., and Park, Z.-Y. (2011). Development of an off-line capillary column IMAC phosphopeptide enrichment method for label-free phosphorylation relative quantification. J. Chromatogr. B. Analyt. Technol. Biomed. Life Sci. *879*, 2991-2997.

Domanitskaya, E. V, Liu, H., Chen, S., and Kubli, E. (2007). The hydroxyproline motif of male sex peptide elicits the innate immune response in Drosophila females. FEBS J. *274*, 5659-5668.

Gruntenko, N.E., Wen, D., Karpova, E.K., Adonyeva, N. V, Liu, Y., He, Q., Faddeeva, N.V, Fomin, A.S., Li, S., and Rauschenbach, I.Y. (2010). Altered juvenile hormone metabolism, reproduction and stress response in Drosophila adults with genetic ablation of the corpus allatum cells. Insect Biochem. Mol. Biol. *40*, 891-897.

Häsemeyer, M., Yapici, N., Heberlein, U., and Dickson, B.J. (2009). Sensory neurons in the Drosophila genital tract regulate female reproductive behavior. Neuron *61*, 511-518.

Isaac, R.E., Li, C., Leedale, A.E., and Shirras, A.D. (2010). Drosophila male sex peptide inhibits siesta sleep and promotes locomotor activity in the post-mated female. Proc. Biol. Sci. *277*, 65-70.

Johns, D., and Marx, R. (1999). Inducible genetic suppression of neuronal excitability. J. Neurosci. *19*, 1691-1697.

Kitamoto, T. (2001). Conditional modification of behavior in Drosophila by targeted expression of a temperature sensitive shibire allele in defined neurons. J. Neurobiol. *47*, 81-92.

Liu, H., and Kubli, E. (2003). Sex-peptide is the molecular basis of the sperm effect in Drosophila melanogaster. Proc. Natl. Acad. Sci. USA *100*, 9929-9933.

Monastirioti, M. (1996). Characterization of Drosophila tyramine hydroxylase isolation of mutant flies lacking octopamine maria. J.

Neurosci. *76*, 3900-3911.

Monastirioti, M. (2003). Distinct octopamine cell population residing in the CNS abdominal ganglion controls ovulation in Drosophila melanogaster. Dev. Biol. *264*, 38-49.

Mount, S.M., and Salz, H.K. (2000). Pre-messenger RNA processing factors in the Drosophila genome. J. Cell Biol. *150*, 37-43.

Nakayama, S., Kaiser, K., and Aigaki, T. (1997). Ectopic expression of sex-peptide in a variety of tissues in Drosophila females using the P[GAL4] enhancer-trap system. Mol. Gen. Genet. *254*, 449-455.

Old, W.M., Meyer-Arendt, K., Aveline-Wolf, L., Pierce, K.G., Mendoza, A., Sevinsky, J.R., Resing, K.A., and Ahn, N.G. (2005). Comparison of label-free methods for quantifying human proteins by shotgun proteomics. Mol. Cell. Proteomics *4*, 1487-1502.

Park, S., Sonn, J.Y., Oh, Y., Lim, C., and Choe, J. (2014). SIFamide and SIFamide receptor defines a novel neuropeptide signaling to promote sleep in _Drosophila. Mol. Cells *37*, 295-301.

Peng, J., Chen, S., Büsser, S., Liu, H., Honegger, T., and Kubli, E. (2005a). Gradual release of sperm bound sex-peptide controls female postmating behavior in Drosophila. Curr. Biol. *15*, 207-213.

Peng, J., Zipperlen, P., and Kubli, E. (2005b). Drosophila sex-peptide stimulates female innate immune system after mating via the Toll and Imd pathways. Curr. Biol. *15*, 1690-1694.

Pfeiffer, B.D., Ngo, T.-T.B., Hibbard, K.L., Murphy, C., Jenett, A., Truman, J.W., and Rubin, G.M. (2010). Refinement of tools for targeted gene expression in Drosophila. Genetics *186*, 735-755.

Rezával, C., Pavlou, H.J., Dornan, A.J., Chan, Y.-B., Kravitz, E.A., and Goodwin, S.F. (2012). Neural circuitry underlying Drosophila female postmating behavioral responses. Curr. Biol. *22*, 1155-1165.

Ribeiro, C., and Dickson, B.J. (2010). Sex peptide receptor and neuronal TOR/S6K signaling modulate nutrient balancing in Drosophila. Curr. Biol. *20*, 1000-1005.

Rodri, O., Lo, I., Labarca, P., Zurita, M., Reynaud, E., and Gene, D. De (2006). Oviduct contraction in Drosophila is modulated by a neural network that is both, octopaminergic and glutamatergic. J. Cell. Physiol. *198*, 183-198.

Sliter, T., Sedlak, B., Baker, F., and Schooley, D. (1987). Juvenile hormone in Drosophila melanogaster: identification and titer determination during development. Insect Biochem. *17*, 161-165.

Tang, J., and Rosbash, M. (1996). Characterization of yeast U1 snRNP A protein: identification of the N-terminal RNA binding domain (RBD) binding site and evidence that the C-terminal RBD functions. RNA *2*, 1058-1070.

Wang, Q., Taliaferro, J.M., Klibaite, U., Hilgers, V., Shaevitz, J.W., and Rio, D.C. (2016). The PSI-U1 snRNP interaction regulates male mating behavior in Drosophila. Proc. Natl. Acad. Sci. USA *113*, 5269-5274

Walker, S.J., Corrales-Carvajal, V.M., and Ribeiro, C. (2015). Postmating circuitry modulates salt taste processing to increase reproductive output in Drosophila. Curr. Biol. *25*, 2621-2630.

Yang, C.-H., Belawat, P., Hafen, E., Jan, L.Y., and Jan, Y.-N. (2008). Drosophila egg-laying site selection as a system to study simple decision-making processes. Science *319*, 1679-1683.

Yang, C.-H., Rumpf, S., Xiang, Y., Gordon, M.D., Song, W., Jan, L.Y., and Jan, Y.-N. (2009). Control of the postmating behavioral switch in Drosophila females by internal sensory neurons. Neuron *61*, 519-526.

Yapici, N., Kim, Y., Ribeiro, C., and Dickson, B. (2008). A receptor that mediates the post-mating switch in Drosophila reproductive behaviour. Nature *451*, 33-38.

Yu, J.Y., Kanai, M.I., Demir, E., Jefferis, G.S.X.E., and Dickson, B.J. (2010). Cellular organization of the neural circuit that drives Drosophila courtship behavior. Curr. Biol. *20*, 1602-1614.

Zhang, Y.Q., Rodesch, C.K., and Broadie, K. (2002). Living synaptic vesicle marker: synaptotagmin-GFP. Genesis *34*, 142-145.

Zhong, L., Hwang, R.Y., and Tracey, W.D. (2010). Pickpocket is a DEG/ENaC protein required for mechanical nociception in Drosophila larvae. Curr. Biol. *20*, 429-434.

Zhu, M.Y., Wilson, R., and Leptin, M. (2005). A screen for genes that influence fibroblast growth factor signal transduction in Drosophila. Genetics *170*, 767-777.